Articles

NMR and Molecular Modeling Investigation of the Mechanism of Activation of the Antitumor Drug Temozolomide and Its Interaction with DNA†

Brian J. Denny,‡ Richard T. Wheelhouse,§ Malcolm F. G. Stevens,*,§ Lincoln L. H. Tsang,‡ and John A. Slack‡

Cancer Research Campaign Experimental Cancer Chemotherapy Group, Cancer Research Laboratories, Department of Pharmaceutical Sciences, University of Nottingham, Nottingham NG7 2RD, U.K., and Pharmaceutical Sciences Institute, Aston University, Birmingham, B4 7ET, U.K.

Received January 24, 1994; Revised Manuscript Received May 5, 1994®

ABSTRACT: The hypothesis that the antitumor prodrug temozolomide is ring-opened to MTIC which then further breaks down to a reactive diazonium ion at guanine-rich sequences in DNA has been probed by NMR spectroscopy and computational techniques. Temozolomide is stable at acid pH but decomposes to MTIC at pH > 7; in contrast, MTIC is stable at alkaline pH values but rapidly fragments in a methylating mode at pH <7. The proximate methylating agent is the reactive methyldiazonium species. Runs of guanine residues represent an accessible nucleophilic microenvironment in DNA which would facilitate the site-specific conversion of the prodrug temozolomide to MTIC possibly via an activated water molecule in the major groove. Molecular modeling of the structure of temozolomide indicates that the prodrug can make a favorable noncovalent encounter with DNA. The known structure–activity relationships as well as the biological and clinical properties of temozolomide can be interpreted in terms of this model.

The antitumor agent temozolomide[1] (**1**) (Figure 1) was selected for clinical trial on the basis that it displayed clear toxicological and mechanistic advantages over the prototype imidazotetrazinone mitozolomide (**2**) (Stevens *et al.*, 1987). The 3-(2-chloroethyl) substituent in mitozolomide is ultimately involved in effecting a cross-linking lesion in DNA (Gibson *et al.*, 1984), and this is probably responsible for the undesirable side effects elicited by the drug, notably thrombocytopenia (Newlands *et al.*, 1985). Temozolomide on the other hand has displayed encouraging activity against brain tumors in preliminary clinical trials when employed in a divided dose schedule (O'Reilly *et al.*, 1993) without toxicological problems.

In a recent paper in this series we presented results on the crystal structure of temozolomide and a molecular modeling study of the rotational characteristics of the 8-carboxamide group (Lowe *et al.*, 1992); the relevance of these structural features to the action of temozolomide as a major-groove-directed prodrug of MTIC (**3**) was explored. In this paper we have attempted to rationalize, by chemical reactivity considerations, ^{1}H-NMR and ^{31}P-NMR studies, and molecular modeling methods, the current state of knowledge of the chemical and biological reactions of temozolomide that have clinical relevance. In particular we have addressed the following facts: (a) the rates of ring-opening of temozolomide and degradation of MTIC are pH dependent; (b) structure–activity studies on imidazotetrazinones show that a hydrogen-bonding-donor group at the C-8 position is required for antitumor activity (Horspool *et al.*, 1990) and that bulky groups at the C-6 position have a dyschemotherapeutic effect (Lunt *et al.*, 1987); (c) MTIC reacts with DNA with a marked specificity for runs of contiguous guanine residues (Gibson *et al.*, 1988).

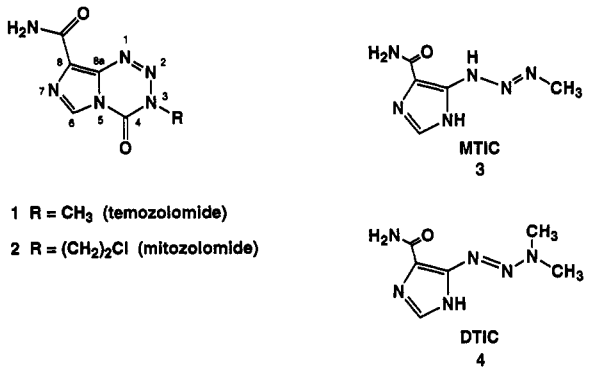

FIGURE 1: Chemical formulas of temozolomide, mitozolomide, MTIC, and DTIC and numbering system of the imidazo[5,1-*d*]-1,2,3,5-tetrazine ring system.

MATERIALS AND METHODS

Drugs and Chemicals. Temozolomide was obtained from the Experimental Cancer Chemotherapy Group, Aston University, Birmingham, U.K., and MTIC was synthesized from the reaction of 5-diazoimidazole-4-carboxamide and methylamine in anhydrous ethyl acetate (Shealy & Krauth, 1966).

† Part 30 of the series "Antitumor Imidazotetrazines". For Part 29 see O'Reilly *et al.* (1993). We are grateful to the Cancer Research Campaign, U.K., for supporting this work.

* Author to whom correspondence should be addressed.
‡ Aston University.
§ University of Nottingham.

® Abstract published in *Advance ACS Abstracts,* June 1, 1994.

[1] Abbreviations: temozolomide, 8-carbamoyl-3-methylimidazo[5,1-*d*]-1,2,3,5-tetrazin-4(3*H*)-one; mitozolomide, 8-carbamoyl-3-(2-chloroethyl)imidazo[5,1-*d*]-1,2,3,5-tetrazin-4(3*H*)-one; MTIC, 5-(3-methyltriazen-1-yl)imidazole-4-carboxamide; DTIC, 5-(3,3-dimethyltriazen-1-yl)imidazole-4-carboxamide; AIC, 5-aminoimidazole-4-carboxamide; DMSO, dimethyl sulfoxide; DMSO-d_6, hexadeuterated dimethyl sulfoxide; MNNG, *N*-methyl-*N'*-nitro-*N*-nitrosoguanidine; TSP, 3-(trimethylsilyl)propionic-2,2,3,3-d_4 acid sodium salt; FID, free induction decay; d, doublet; q, quartet; *J*, coupling constant.

0006-2960/94/0433-9045$04.50/0

Diazomethane was prepared using a Wheaton millimole scale MNNG apparatus purchased from the Aldrich Chemical Co. (Black, 1983). In the outer tube was placed 0.5 mL of the solution to be reacted with diazomethane (0.2 M phosphate buffer in D_2O or 10% sodium carbonate in D_2O) with a magnetic flea; in the inner tube was placed 0.4 mL of H_2O and 100 mg (0.68 mmol) of MNNG. The apparatus was sealed and placed in an ice bath. Over half an hour 0.5 mL of 5 M sodium hydroxide in H_2O was added to the inner tube via a syringe, the substrate solution was stirred vigorously throughout. At the end of the addition the reaction mixture was left to stand on ice for 1 h and then opened to the atmosphere and allowed to stand overnight. The ^{1}H-NMR spectrum (with presaturation of the HOD peak) was then recorded.

Methyl phosphate was prepared by hydrolysis of methyl dichlorophosphate. In a 5 mm diameter NMR tube was placed a solution of 107 mg (1 mmol) of sodium carbonate in 1 mL of D_2O; 0.1 mL (1 mmol) of methyl dichlorophosphate was added. When the effervescence had subsided, the final pH of the solution was about 1; the ^{1}H- and ^{31}P-NMR spectra were recorded: δ_H 3.55 (d, J_{PH} = 11 Hz); δ_P 6.1 (q, J_{PH} = 11 Hz). The solution was then used to spike other samples where proof of the presence of methyl phosphate was required.

Dimethyl phosphate was prepared by cleavage of trimethyl phosphate (Zervas & Dilaris, 1955). A solution of trimethyl phosphate (2 mL, 17 mmol) and sodium iodide (2.83 g, 19 mmol) in 30 mL of acetone was heated under reflux for 1.5 h. On cooling, white crystals of the sodium salt of dimethyl phosphate were formed: these were collected by filtration, washed with more acetone, and dried *in vacuo* to yield 1.8 g (71%); $\delta_H(D_2O)$ 3.57 (d, J_{PH} = 11 Hz); δ_P 8.1 (septet, J_{PH} = 11 Hz).

Stability Studies. Stock solutions (10 mg/mL) of temozolomide and MTIC were prepared in DMSO. Aliquots (10 μL) of the solutions were added to silica cuvettes (1 cm path length) containing 0.1 M buffer solutions maintained at 37 °C. The buffer solutions were the following: acid phthalate buffer (pH 3–4); neutralized phthalate buffer (pH 5–6); phosphate buffer (pH 7–8); and alkaline borate buffer (pH 9–10). The decreases in absorbance with time at 328 (temozolomide) and 316 nm (MTIC) were measured using a Hewlett Packard HP 8451A diode array ultraviolet spectrometer. No measurable differences in pH of the solutions were detected before and after each decomposition experiment.

NMR Studies. NMR spectra were recorded on Bruker AC250 (kinetics and ^{31}P experiments) and Bruker ARX250 (all other spectra) spectrometers observing ^{1}H at 250.13 MHz and ^{31}P at 101.26 MHz. Typical conditions were as follows.

For proton kinetic experiments, blocks of 32 transients were recorded with a spectral width of 2.5 kHz, a 30° observe pulse was used, and the data were collected as 32K data points. There was no relaxation delay; 0.1 Hz exponential multiplication was applied to the FID before transformation to 32K real data points, and the DMSO peak δ 2.5 was used for referencing.

Other proton spectra were recorded with presaturation of the HOD peak using the Bruker pulse program zg0pr with the center of the spectrum set to the HOD peak. The spectral width was 3 kHz, and the presaturation pulse was applied for 2 s during the relaxation delay at a transmitter power attenuation of 45 dB from maximum. The observe pulse width was 30°, and the data were collected as 32K data points transformed to 32K real data points after application of a Gaussian window function (0.2 Hz Gaussian, −0.2 Hz exponential line broadening). TSP was used as internal reference.

^{31}P spectra were recorded with a spectral width of 6 kHz, using a 30° observe pulse and relaxation delay of 0.5 s between transients; the data were collected as 32K data points transformed to 32K real points after application of 1.0 Hz exponential line broadening. The reference was external 85% phosphoric acid; spectra were recorded with and without ^{1}H decoupling.

For the kinetics experiment 0.2 M phosphate buffer (0.5 mL) in D_2O (pD 7.8; equivalent to pH 7.4) was placed in a 5 mm diameter NMR tube and warmed to 37 °C. A solution of temozolomide (**1**) (0.1 mL of a solution of 40 mg/mL in DMSO-d_6 at 37 °C) was added, the tube placed in the probe, thermostated at 37 °C, and the magnet shimmed. The Bruker program KINETICS.AU was used to record spectra at 0.5 h intervals for 14 h, by which time all **1** had reacted. Two drops of 10 M DCl in D_2O were added, and the ^{31}P-NMR spectra were recorded with and without ^{1}H decoupling. Authentic methyl and dimethyl phosphate were added, and both ^{1}H and ^{31}P spectra were re-run: enhancement of peak intensities allowed unequivocal assignment of the product peaks.

For the MTIC hydrolysis, 0.5 mL of 10% sodium carbonate in D_2O was placed in a 5 mm NMR tube and warmed to 37 °C; 0.1 mL of a solution of authentic MTIC (17 mg/mL in DMSO-d_6 equimolar with the solution of **1** used above) was added. After 3 h, the ^{1}H-NMR spectrum was recorded; after 12 h, no MTIC remained. The experiment was repeated using 10% sodium carbonate in 1:1, 3:1, and 9:1 mixtures of H_2O/D_2O.

Molecular Modeling. The co-ordinates of the DNA used in the study were those of idealized B-DNA (Arnott *et al.*, 1983). The base sequence ACTTACGGGCTACCT was constructed along with its complementary strand using the program GENHELIX (Neidle & Pearl, 1987) and transferred to the molecular modeling package INSIGHT2.2 (marketed and distributed by Biosym Technologies Ltd., San Diego, CA) running on a Silicon Graphics Iris-Indigo workstation. Partial charges were then calculated using the molecular mechanics program AMBER (Weiner *et al.*, 1984). For all the AMBER energy calculations with temozolomide and DNA, explicit solvent molecules were excluded and a distance-dependent dielectric of 4 was used; the 1–4 interactions were scaled by 0.5. The van der Waals and electrostatics cutoff distance was 10 Å. For the solvent-accessible surface calculations, the modeling package QUANTA (MSI, Waltham, MA) was used with a probe radius of 1.4 Å. The modeling package CHEMX (Chemical Design Ltd., Oxford, U.K.) running on a VAX 8650 was used for all of the small molecule modeling. For the *ab initio* calculations GAMESS (Schmidt *et al.*, 1990) was used with the 321-G basis set. The crystal structure of temozolomide was as determined by Lowe *et al.* (1992).

RESULTS AND DISCUSSION

Chemical Stability of Temozolomide and MTIC. The stability of temozolomide and MTIC in aqueous buffers over the pH range 4–10 was monitored by diode array UV spectrophotometry. Degradation of both drugs is pH-sensitive (Figure 2) but whereas the prodrug temozolomide is stable at acidic pH values and labile above pH 7, exactly the converse obtains with the ring-opened species MTIC, which is unstable below pH 7 but more stable at alkaline pH values. Temozolomide has a half-life of 1.83 h at 37 °C in phosphate buffer (0.1 M) at pH 7.4 as determined in the present work, whereas

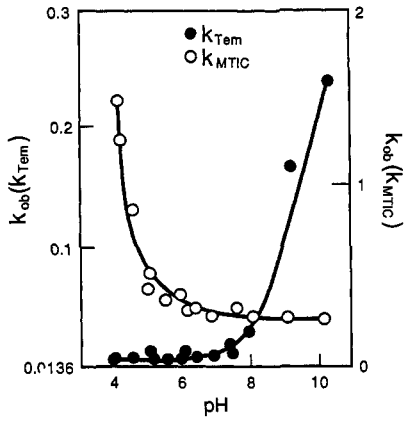

FIGURE 2: Plot of stability constant (k_{ob}) versus pH of temozolomide (Tem) and MTIC.

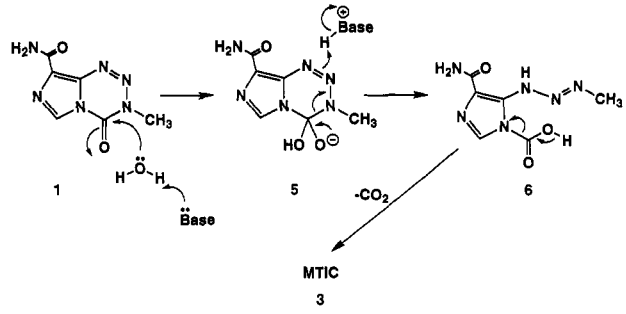

FIGURE 3: Reaction scheme for the base-catalyzed decomposition of temozolomide to MTIC in water.

MTIC has a half-life of approximately 2 min at the same pH. Interestingly, the mean plasma half-life of temozolomide in a group of patients undergoing intravenous and oral dosing (n = 34) was 1.81 h (Newlands *et al.*, 1992). This implies that metabolism has little or no impact on the distribution and elimination of the prodrug: in contrast, generation of the bioactive agent MTIC from the structurally related prodrug DTIC (**4**) is not under chemical control and is subject to the vagaries of metabolism (Tsang *et al.*, 1991). Clearly, there will be only a small pH window around physiological pH at which the propensity of temozolomide to undergo ring-opening is matched by the breakdown of the MTIC in a methylating mode. The balance of these processes could critically influence the reactivity of temozolomide and MTIC in different intra- and intercellular compartments.

Mechanism of Ring-Opening of Temozolomide to MTIC. The greatest positive charge (+0.417) in the tetrazinone ring of temozolomide is located at the carbonyl C-4 position as calculated by the *ab initio* quantum mechanics package GAMESS using a 321-G basis set. Therefore, this site will be most vulnerable to nucleophilic attack by water. The proposed mechanism of activation of temozolomide (Figure 3) is consistent with experimental evidence. Base-catalyzed orthogonal attack by a water molecule at C-4 leads to a tetrahedral adduct **5**, which undergoes ring-opening to give an unstable carbamic acid **6**: this intermediate loses carbon dioxide to afford MTIC (**3**). In alkaline conditions (10% aqueous sodium carbonate) MTIC is relatively stable, and the reaction can be terminated at this point (Stevens *et al.*, 1987). Monomethyltriazenes are known to be unstable in acidic conditions and methylate nucleophiles (Vaughan & Stevens, 1978); MTIC clearly exhibits this instability (Figure 2).

NMR Studies on the Decomposition of Temozolomide. When the decomposition of temozolomide was monitored by ^{1}H-NMR spectroscopy in deuterated phosphate buffer at pD 7.8 (equivalent to pH 7.4), the imidazole proton region of the spectra was dominated by signals from the (deuterated) starting material (δ 8.6) and deuterated AIC (δ 7.23), indicating that there is little buildup of other imidazole species (Figure 4). The rate-determining step in the overall decomposition at pH 7.4 must be at an early stage of the reaction pathway, probably the base-catalyzed addition of water to temozolomide.

The methyl group region of the spectrum is of considerable mechanistic significance. Methanol and methyl phosphate were formed in the ratio 1:1.6, and a trace of dimethyl phosphate was detected. The phosphorus-containing products and methanol were identified by spiking the sample with authentic methyl and dimethyl phosphate or methanol, re-running the ^{1}H- and ^{31}P-NMR spectra, and observing the enhancements of peak intensity. The integrity of the methyl group was corrupted by isotopic exchange of deuterium for hydrogen, and signals attributable to CH_3, CH_2D, and CHD_2 were seen in the same proportions in the methanol and methyl phosphate products (Figure 5a). Reaction of authentic MTIC in 10% sodium carbonate in D_2O (conditions under which it decomposes slowly) allowed for simultaneous observation of MTIC and the final products of methyl group transfer. While the MTIC signal (δ 3.16) remained a sharp singlet (i.e.,

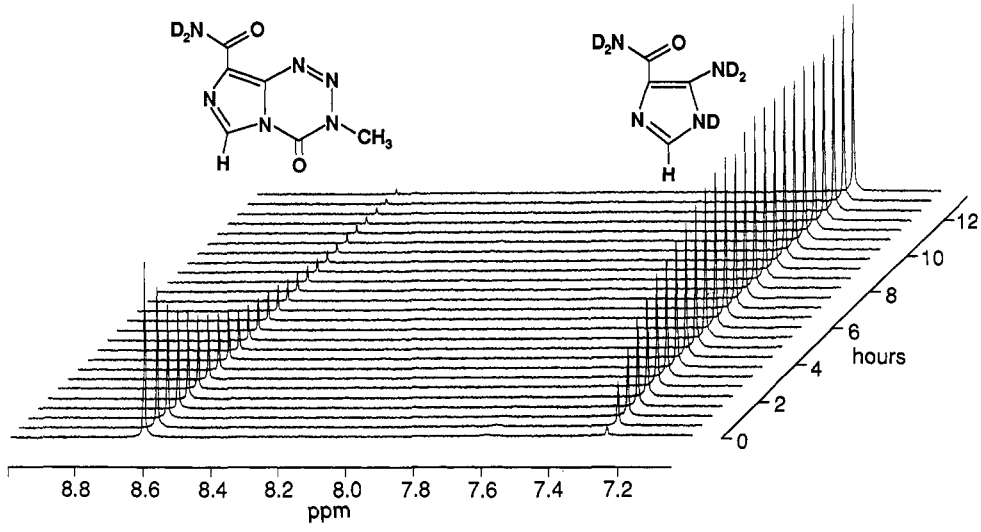

FIGURE 4: Aromatic region of the ^{1}H-NMR spectra of the decomposition of temozolomide in deuterated phosphate buffer at pD 7.8.

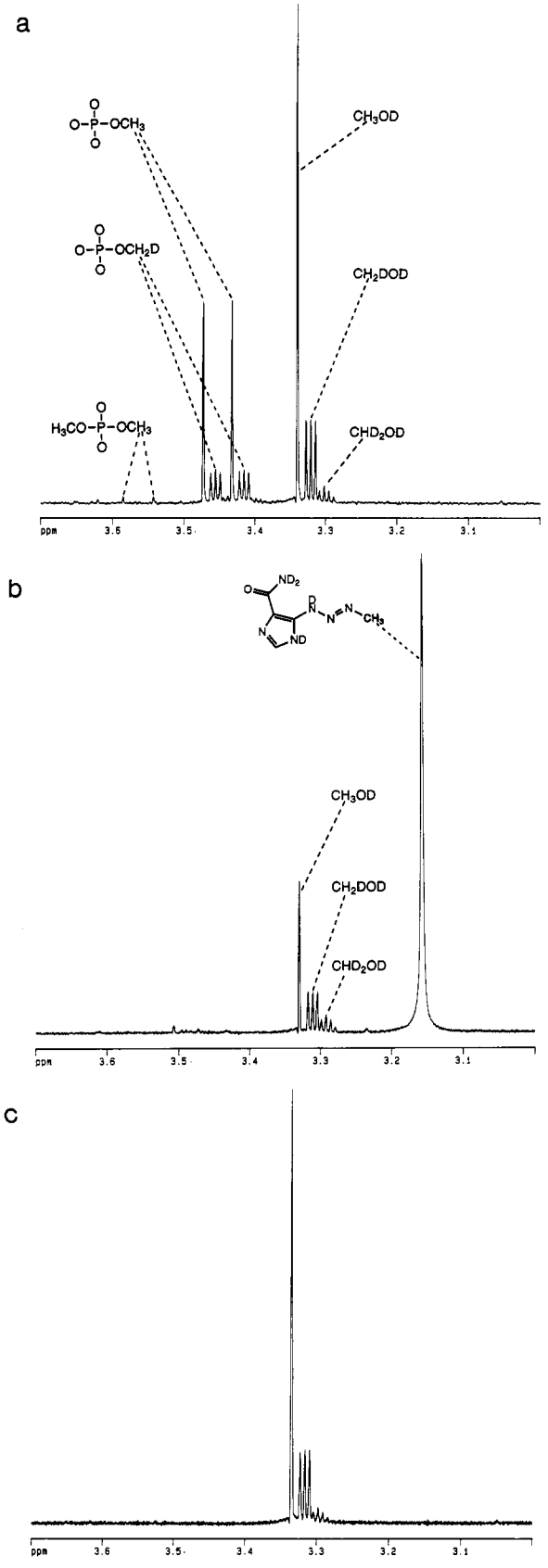

FIGURE 5: (a, top) Methyl region of the ^{1}H-NMR spectrum of the decomposition of temozolomide in deuterated phosphate buffer at pD 7.8. (b, middle) Methyl region of the ^{1}H-NMR spectrum of the decomposition of MTIC in 10% sodium carbonate–D_2O. (c, bottom) Methyl region of the ^{1}H-NMR spectrum of the decomposition of diazomethane in 10% sodium carbonate–D_2O.

unexchanged), the methylated products showed the same degree of deuterium incorporation as seen before (Figure 5b).

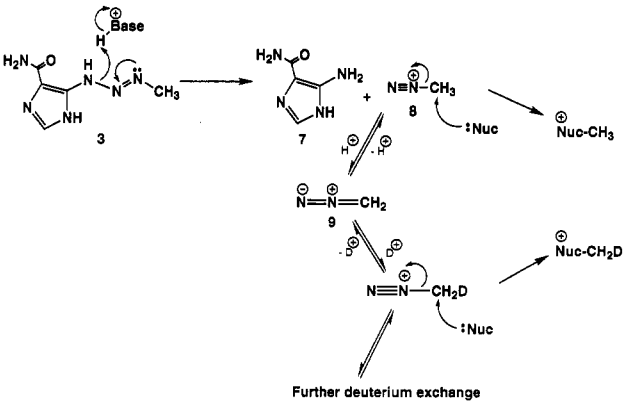

FIGURE 6: Reaction scheme for the decomposition of MTIC in deuterated phosphate buffer at pD 7.8.

It was also shown that the extent of deuterium incorporation depended on the ratio of exchangeable H/D in the solvent.

Clearly, this new information is not compatible with our original working hypothesis in which we proposed that MTIC itself was the methylating agent (Clark *et al.*, 1990; Lowe *et al.*, 1992) and is suggestive of the discrete intervention of a further intermediate in the reaction pathway in which the methyl group is able to equilibrate with the population of exchangeable H/D in the solvent. Such an intermediate must be the methyldiazonium cation **8** formed in a unimolecular fragmentation of protonated (or protonating) MTIC with liberation of AIC **7** (Figure 6). Loss of a proton from **8** affords diazomethane **9**, which can protonate (deuterate) to account for the observed pattern of isotopic exchange. Support for this proposal came from an experiment in which diazomethane was decomposed in sodium carbonate in D_2O; the same pattern of deuterium incorporation into the methanol was observed (Figure 5c). Similar deuterium exchange has been observed in the methyl group of the methyldiazonium species formed in the decompositions of 1,3,3-trimethyltriazene, *N*–methyl-*N*-(nitrosoethyl)carbonate, *N*-(acetoxymethyl)-*N*-nitrosomethylamine, and *N*-methyl-*N*-nitrosourea in deuterated phosphate buffer (Smith *et al.*, 1985, 1986).

Noncovalent Binding of Temozolomide to DNA. Guanine bases in DNA have a more negative molecular electrostatic potential than other bases (Pullman & Pullman, 1981), and the atom with the most negative potential is the N-7 of guanine. This explains why this atom is the most frequently alkylated by a series of electrophilic drugs (Richardson *et al.*, 1987). Semiquantitative analysis using the molecular modeling packages PIMMS (Oxford Molecular Ltd., Oxford, U.K.) with the empirical charge calculation system CHARGE2 (Abrahams *et al.*, 1988) and QUANTA using the Charge Templates method of calculating charges show that a run of three consecutive guanines has a higher dipole moment than other sequences of bases: this is consistent with the expectation of enhanced nucleophilicity of this major-groove microenvironment and its associated water molecules. The second factor responsible for the selectivity of guanine alkylation is the steric accessibility of guanine in the major groove (Lavery *et al.*, 1981).

The solvent-accessible (Connolly) surface of different atoms in B-DNA was calculated with QUANTA using a probe radius of 1.4 Å; this is the radius of a water molecule. The data recorded in Table 1 are the mean of at least three different determinations of potential electrophile-acceptor atoms. The electrostatic potentials of the different atoms are also shown (Pullman & Pullman, 1981). The N-7 of guanine is the most accessible and has the greatest negative potential. When calf

Table 1: Steric Surface Area Accessibilities and Potentials of Atoms in B-DNA

atom	accessibility (Å^2)	potential[a] (kcal mol^{-1})	groove
N7 (gua)	10	−683	major
O6 (gua)	8	−654	major
N7 (ade	8	−650	major
O4 (thy)	3	−612	major
O2 (thy)	7	−663	minor
N3 (ade)	2	−668	minor
O2 (cyt)	4	−645	minor
N3 (gua)	2	−670	minor

[a] The potential minima situated closest to particular atoms was calculated using *ab initio* SCF methods. The calculations were simplieifed by using an overlap multipole expansion of the electron density [taken from Pullman and Pullman (1981)].

thymus DNA was treated with ^{14}C-labeled temozolomide, 70% of the label was associated with N-7 of guanine, 5% with O-6 of guanine, and 25% with other sites (V. Bull and M. J. Tisdale, personal communication, 1990). These data are consistent with the steric accessibility and electrostatic potentials shown in Table 1. Although temozolomide may well bind noncovalently throughout the major groove of DNA, the molecular modeling studies predict that both ring-opening of the prodrug temozolomide to MTIC and methylation of DNA by the methyldiazonium reactive intermediate are facilitated by the basic microenvironment of guanine-rich sequences. Preferential reaction of MTIC at guanine N-7 residues in runs of guanine residues has been confirmed experimentally (Gibson *et al.*, 1988).

The starting point for the modeling studies was the crystal structure of temozolomide (Lowe *et al.*, 1992), which was docked into the major groove of DNA at the run of three guanines in the sequence ACTTACG$_1$G$_2$G$_3$CTACCT. The position of the drug molecule was adjusted until the most favorable interaction was obtained. The complex was minimized with the molecular mechanics program AMBER (steepest descents 3000 cycles, conjugate gradient 5000 cycles) until an RMS gradient of less than 0.0001 kcal/Å was obtained. During the minimization the carboxamide group was constrained to planarity with respect to the imidazole ring (Lowe *et al.*, 1992). This proposed (noncovalent) binding of temozolomide to DNA is shown as a overview (Figure 7) and in detail (Figure 8a), the latter showing the hydrogen-bonding contact distances between the DNA and temozolomide molecules. In this orientation the carboxamide amino group is H-bonded to the O-6 and N-7 of G$_1$ and the carbonyl oxygen to the 4-amino group of C$_3$. In addition, the N-1 of temozolomide can act as an H-bond acceptor for a hydrogen atom of the 4-amino group of C$_3$. A water molecule can be positioned such that is forms hydrogen bonds bridging the 3.3 or 3.5 Å distance between the O-6 and N-7 atoms, respectively, of G$_3$. This "activated" water is in an ideal location for orthogonally directed nucleophilic attack at C-4 of temozolomide (Figure 8b).

An important feature of the model is that it envisages the crucial reactions of temozolomide in the major groove occur shielded from competition by other nucleophiles, and this is consistent with the known structure–activity relationships in imidazotetrazine derivatives (Stevens, 1987). If the 3-methyl group of temozolomide is replaced by the 3-(2-chloroethyl) group in mitozolomide, there is no appreciable change in binding. Previously we have shown that antitumor activity in mitozolomide analogues **2** against murine tumor systems decreases when bulky substituents are placed at the C-6 position and that a hydrogen-bonding donor group at C-8 is

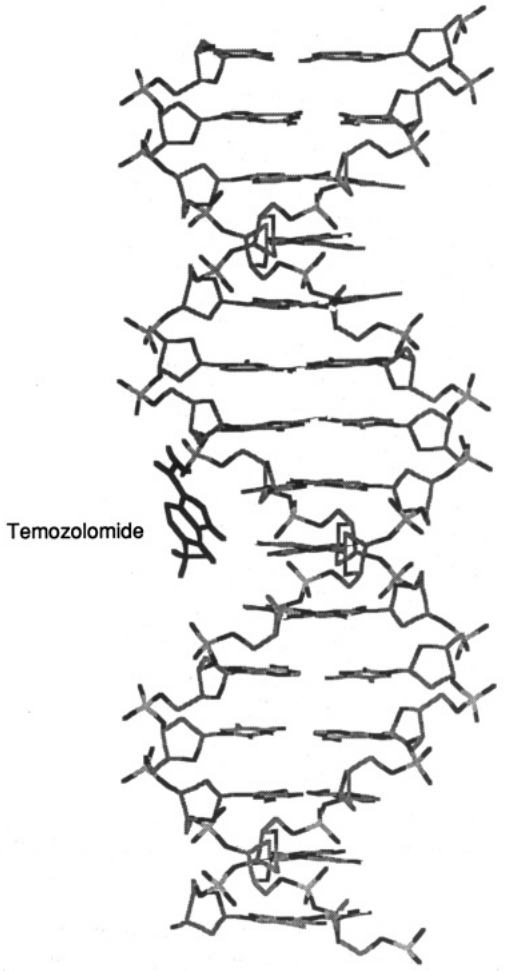

FIGURE 7: Overview of temozolomide bound to DNA in the major groove.

preferred (Lunt *et al.*, 1987). If this relationship is also applicable in the 3-methyl (temozolomide) series, substituents other than hydrogen at C-6 would have only minor effects on the calculated atomic charge at C-4, which ranges from +0.410 to +0.420 for a series of 6-alkyl- and 6-aryl-3-methylimidazotetrazinones (Table 2). Also, the calculated steric accessibility of a water molecule probe at C-4 in a series of 6-substituted congeners of temozolomide is little influenced by the bulk of the 6-substituent. Thus, there is no electronic or steric reason why the ring-opening at C-4 should not still occur. Any substituent larger than H at C-6 would interact sterically with H-8 of G$_2$ (Figure 8a) and have the effect of destabilizing the orientating influence of the hydrogen bonds between the DNA and the 8-carboxamide group of active imidazotetrazines.

It is predicted by the model that temozolomide may exhibit an enhanced DNA sequence selectivity compared with other alkylating agents. In several respects temozolomide most closely resembles the promutagen *N*-methyl-*N*-nitrosourea, which also does not require metabolic activation but is chemically activated at pH 7.4 in aqueous media to generate a methyldiazonium species (Smith *et al.*, 1985; Bleasdale *et al.*, 1991). However the nitrosourea lacks the imidazole-carboxamide residue which may impart additional recognition capability to temozolomide through hydrogen-bonding interactions. Furthermore, although the final methylation of DNA from both agents may be via an identical S$_N$2 mechanism, the nature of the leaving groups which also have to be accommodated within the major groove is different.

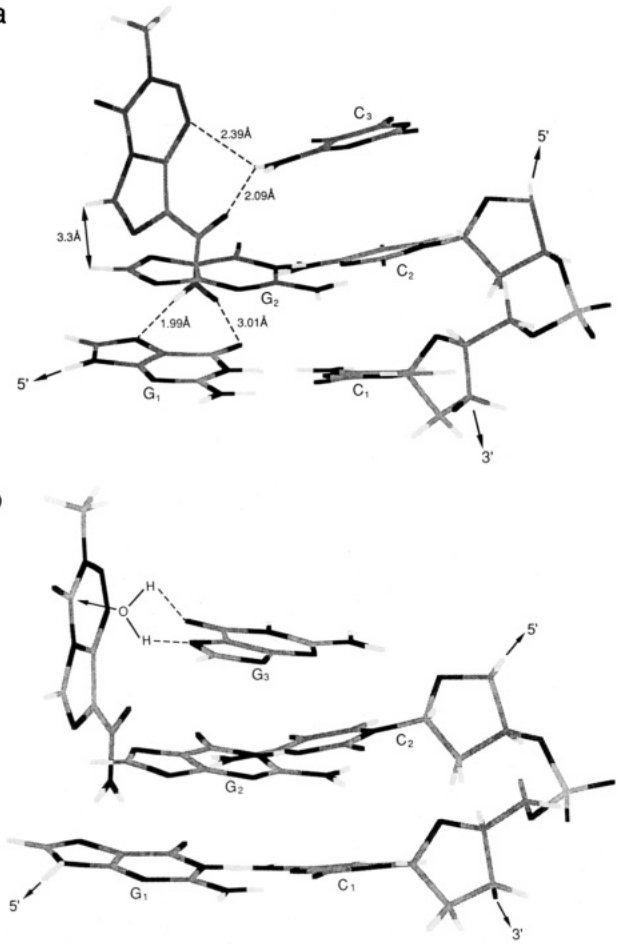

FIGURE 8: (a, top) Potential hydrogen-bonding interactions (- - -) in the noncovalent association of temozolomide and a GGG sequence in the major groove of DNA and the H–H distance (↔) between H-6 of temozolomide and H-8 of guanine. (b, bottom) Nucleophilic attack at C-4 of temozolomide by an "activated" water molecule.

Table 2: Calculated Effects of Substituents at C-6 of 3-Methylimidazotetrazines on Charge and Accessibility at C-4

substituent at C-6 in 3-methylimidazotetrazines	charge at C-4[a]	accessibility[b] (Å²)
H (temozolomide **1**)	0.417	9
methyl	0.419	9
ethyl	0.418	8
isopropyl	0.420	7
phenyl	0.417	8
cyclohexyl	0.410	7

[a] Calculated with the *ab initio* quantum mechanics package GAMESS with the 321-G basis set. [b] Calculated with the molecular modeling package QUANTA with a water molecule as probe (1.4 Å radius).

The clinical activity of orally administered temozolomide against glioma (O'Reilly *et al.*, 1993) may be accounted for, in part, by the pH stability data presented in Figure 2. The robust stability of temozolomide at acidic pH (and its lipophilicity) allows for excellent oral bioavailability (Newlands *et al.*, 1992) and presumably penetration of the blood–brain barrier; the activity against brain tumors is not exhibited by other clinically used prodrugs of MTIC (Meer *et al.*, 1986). A number of authors (Rottenberg *et al.*, 1984; Vaupel *et al.*, 1989) have demonstrated a pH gradient between healthy brain tissue (pH 6.96–7.05) and glioma (7.15–7.22). These differences, though small, could contribute to the selective toxicity of temozolomide toward glioma cells: the lower pH of healthy tissue would stabilize the prodrug and favor passage of the intact prodrug to the tumor tissue. However, it is important to note that other factors—such as the activity of DNA repair enzymes (Baer *et al.*, 1993)—also influence the susceptibility of tumors to temozolomide.

ACKNOWLEDGMENT

We are grateful to Prof. A. Gescher of The University of Leicester, U.K. and Dr. S. Freeman and Dr. C. H. Schwalbe of Aston University, U.K., for helpful discussions. We thank Dr. C. A. Laughton, Institute of Cancer Research, Sutton, U.K., for supplying the GENHELIX program and Biosym Inc., U.K., for the use of extra modules of the INSIGHT molecular modeling package.

REFERENCES

Abrahams, R. J., & Smith, P. E. (1988) *Nucleic Acids Res. 16*, 2639–2657.

Arnott, S., Chandrasekaran, R., Hall, I., & Puigjaner, L. C. (1983) *Nucleic Acids Res. 11*, 4145–4155.

Baer, J. C., Freeman, A. A., Newlands, E. S., Watson, A. J., Rafferty, J. A., & Margison, G. P. (1993) *Br. J. Cancer 67*, 1299–1302.

Black, T. H. (1983) *Aldrichimica Acta 16*, 3–10.

Bleasdale, C., Golding, B. T., McGinnis, J., Muller, S., & Watson, W. P. (1991) *J. Chem. Soc., Chem. Commun.*, 1726–1728.

Citron, M., Decker, R., Chen, S., Schneider, S., Graver, M., Kleynerman, L., Kahn, L. B., White, A., Schoenhaus, M., & Yarosh, D. (1991) *Cancer Res. 51*, 4131–4134.

Clark, A. S., Stevens, M. F. G., Sansom, C. E., & Schwalbe, C. H. (1990) *Anti-Cancer Drug Des. 5*, 63–68.

Gibson, N. W., Hickman, J. A., & Erickson, L. C. (1984) *Cancer Res. 44*, 1772–1775.

Gibson, N. W., Hartley, J. A., Lafrance, R. J., & Vaughan, K. (1988) *Carcinogenesis 9*, 669–674.

Horspool, K. R., Stevens, M. F. G., Newton, C. G., Lunt, E., Walsh, R. J. A., Pedgrift, B. L., Baig, G. U., Lavelle, F., & Fizames, C. (1990) *J. Med. Chem. 33*, 1393–1399.

Lavery, R., Pullman, A., & Pullman, B. (1981) *Int. J. Quantum Chem. 20*, 49–62.

Lowe, P. R., Sansom, C. E., Schwalbe, C. H., Stevens, M. F. G., & Clark, A. S. (1992) *J. Med. Chem. 35*, 3377–3382.

Lunt, E., Newton, C. G., Smith, C., Stevens, G. P., Stevens, M. F. G., Straw, C. G., Walsh, R. J. A., Warren, P. J., Fizames, C., Lavelle, F., Langdon, S. P., & Vickers, L. M. (1987) *J. Med. Chem. 30*, 357–365.

Meer, L., Janzer, R. C., Kleihues, P., & Kolar, G. F. (1986) *Biochem. Pharmacol. 35*, 3243–3247.

Neidle, S., & Pearl, L. H. (1987) GENHELIX: A program for the generation of coordinates for A- and B-form DNA, Institute of Cancer Research, Sutton, Surrey, U.K.

Newlands, E. S., Blackledge, G., Slack, J. A., Goddard, C., Brindley, C. J., Holden, L., & Stevens, M. F. G. (1985) *Cancer Treatment Rep. 69*, 801–805.

Newlands, E. S., Blackledge, G. R. P., Slack, J. A., Rustin, G. J. S., Smith, D. B., Stuart, N. S. A., Quarterman, C. P., Hoffman, R., Stevens, M. F. G., Brampton, M. H., & Gibson, A. C. (1992) *Br. J. Cancer 65*, 287–291.

O'Reilly, S. M., Newlands, E. S., Glaser, M. G., Brampton, M., Rice-Edwards, J. M., Illingworth, R. D., Richards, P. G., Kennard, C., Colquhoun, I. R., Lewis, P., & Stevens, M. F. G. (1993) *Eur. J. Cancer 29A*, 940–942.

Pullman, A., & Pullman, B. (1981) *Q. Rev. Biophys. 14*, 289–380.

Richardson, K. K., Richardson, F. C., Crosby, R. M., Swernberg, R. A., & Skopek, T. R. (1987) *Proc. Natl. Acad. Sci. U.S.A. 84*, 344–348.

Rottenberg, D. A., Ginos, J. Z., Kearfoot, K. J., Junck, L., & Bigner, D. D. (1984) *Ann. Neurol. 15*, S98–S102.

Schmidt, M. W., Balfridge, K. K., Boatz, J. A., Jensen, J. H., Koseki, S., Gordon, M. S., Nguyen, K. A., Windus, T. L., & Elbert, S. T. (1990) *QCPE Bull. 10*, 52–54.

Shealy, Y. F., & Krauth, D. A. (1966) *J. Med. Chem. 9*, 34–38.

Smith, R. H., Koepke, S. R., Tondeur, Y., Denlinger, C. L., & Michejda, C. J. (1985) *J. Chem. Soc., Chem. Commun.*, 936–937.

Smith, R. H., Denlinger, C. L., Kupper, R., Mehl, A. F., & Michejda, C. J. (1986) *J. Am. Chem. Soc. 108*, 3726–3730.

Stevens, M. F. G. (1987) in *New Avenues in Developmental Cancer Chemotherapy*, pp 335–354, Academic Press, London.

Stevens, M. F. G., Hickman, J. A., Langdon, S. P., Chubb D., Vickers, L., Stone, R., Baig, G., Goddard, C., Gibson, N. W., Slack, J. A., Newton, C., Lunt, E., Fizames, C., & Lavelle, F. (1987) *Cancer Res. 47*, 5846–5852.

Tsang, L. L. H., Quarterman, C. P., Gescher, A., & Slack, J. A. (1991) *Cancer Chemother. Pharmacol. 27*, 342–346.

Vaughan, K., & Stevens, M. F. G. (1978) *Chem. Soc. Rev. 7*, 377–397.

Vaupel, P., Kallinowski, F., & Okunieff, P. (1989) *Cancer Res. 49*, 6449–6465.

Weiner, S. J., Kollman, P. A., Case, D. A., Singh, U. C., Ghio, C., Alagona, G., Profeta, S., Jr., & Weiner, P. (1984) *J. Am. Chem. Soc. 106*, 765–784.

Wheelhouse, R. T., & Stevens, M. F. G. (1993) *J. Chem. Soc., Chem. Commun.*, 1178–1179.

Zervas, L., & Dilaris, I. (1955) *J. Am. Chem. Soc. 77*, 5354–5356.